Supporting Information

Impact of Alkyl Chain Length and Water on the Structure and Properties of 1-alkyl-3-methylimidazolium Chloride Ionic Liquids

Paridhi Sanchora[†], Deepak K. Pandey[†], Hardik L. Kagdada[†], Arnulf Materny[$] and Dheeraj K. Singh[†*]

[†]*Department of Physics, Institute of Infrastructure Technology Research and Management, Ahmedabad, 380026, India*
[$]*Department of Physics and Earth Sciences, Jacobs University Bremen, Bremen, 28759, Germany*

*Corresponding author: dheerajsingh84@gmail.com

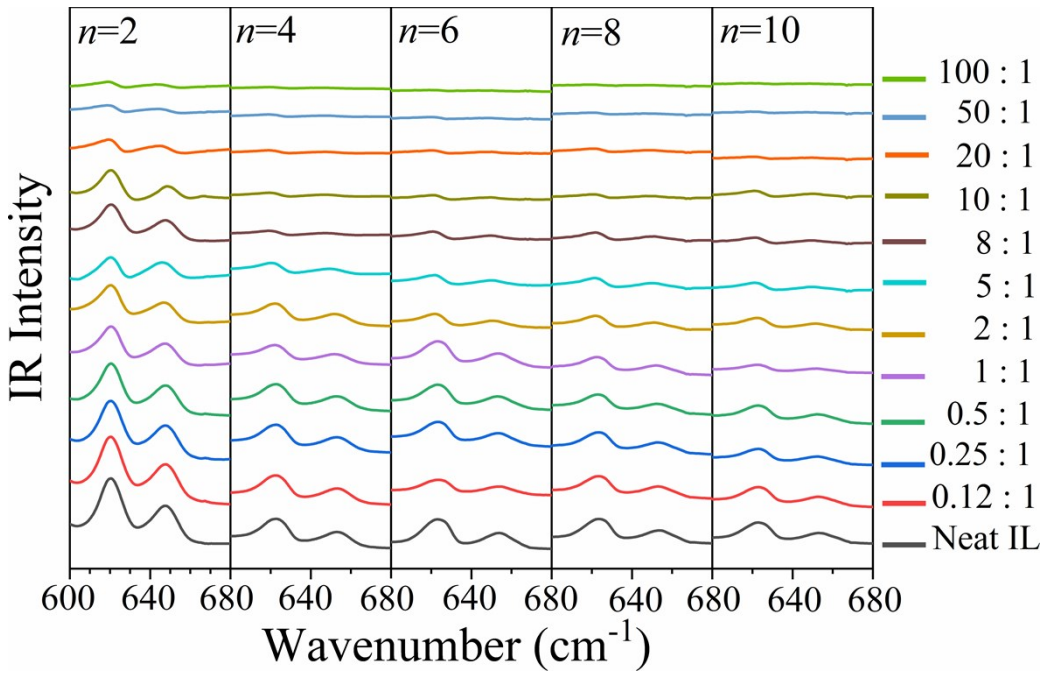

Fig. S1 ATR-IR absorption spectra of neat $C_n$mim Cl (n = 2, 4, 6, 8, 10) ion pairs and their binary mixtures with H_2O in the region of 600-680 cm^{-1} at various H_2O : IL molar ratios. The lines at 623 and 654 cm^{-1} are assigned to ring stretching vibration and alkyl chain N-CH_2-CH_3 asymmetric bending, respectively.

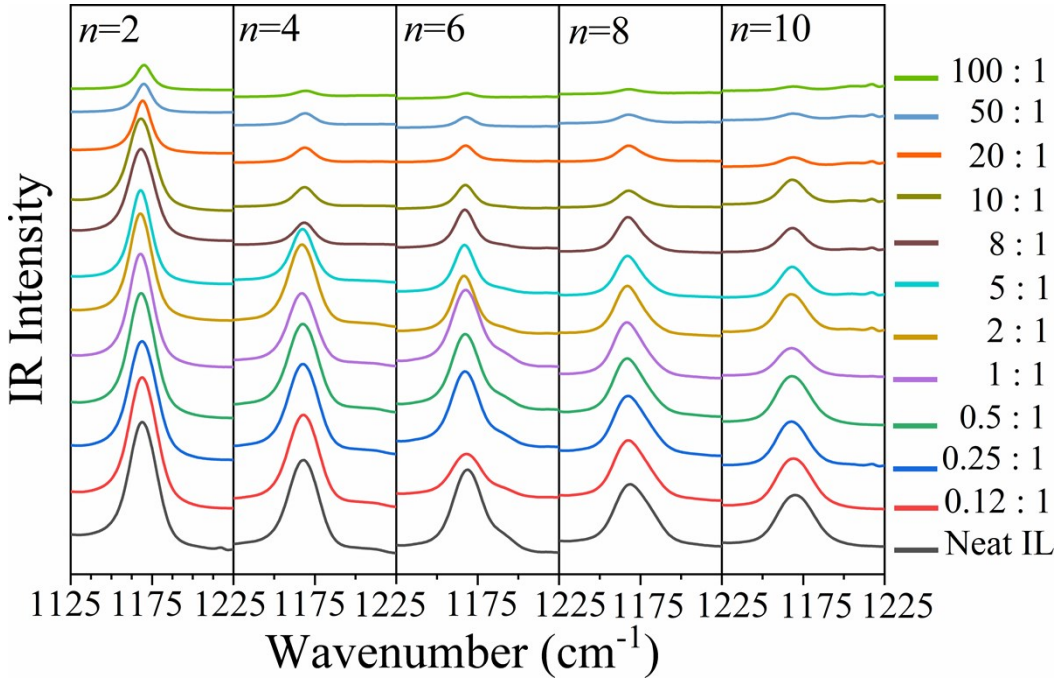

Fig. S2 ATR-IR absorption spectra of neat $C_n$mim Cl (n = 2, 4, 6, 8, 10) ion pairs and their binary mixtures with H_2O in the region of 1125-1225 cm^{-1} at various H_2O : IL molar ratios. The line at 1167 cm^{-1} is assigned to the C-C stretching vibration of the ring.

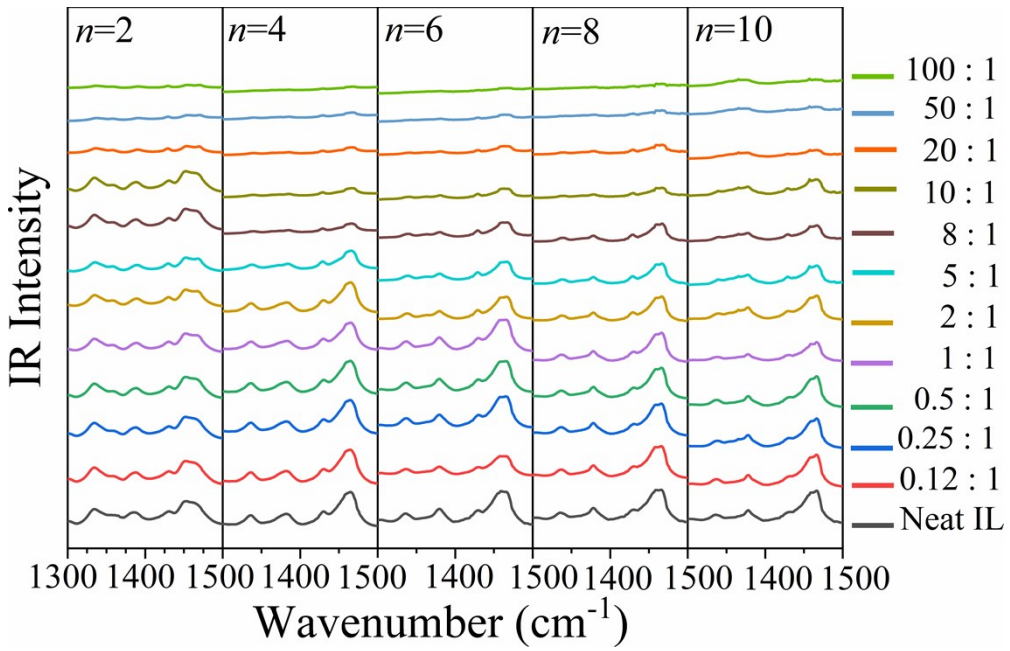

Fig. S3 ATR-IR absorption spectra of neat $C_n$mim Cl (n = 2, 4, 6, 8, 10) ion pairs and their binary mixtures with H_2O in the region of 1300-1500 cm^{-1} at various H_2O : IL molar ratios. The line at 1325 cm^{-1} assigned to the ring C-H in plane bending. The line at 1378 cm^{-1} belongs to the alkyl chain (CH_2) stretching. The peaks at 1453 and 1470 cm^{-1} are assigned to the asymmetric ring stretching and asymmetric bending vibrations of C8-H, respectively.

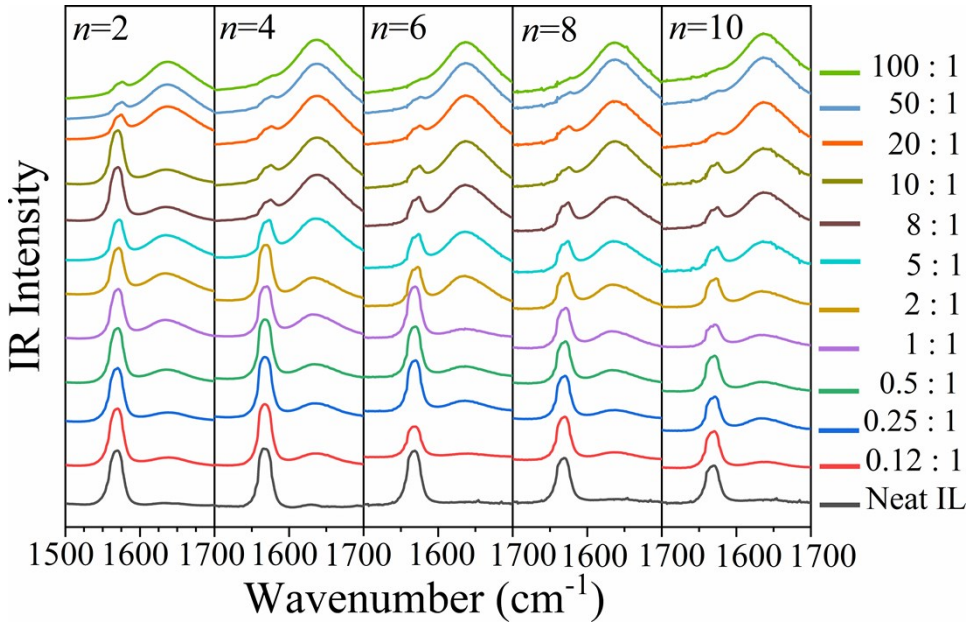

Fig. S4 ATR-IR absorption spectra of neat $C_n$mim Cl (n = 2, 4, 6, 8, 10) ion pairs and their binary mixtures with H_2O in the region of 1500-1700 cm^{-1} at various H_2O : IL molar ratios. The line at 1569 cm^{-1} is assigned to the $C8H_2$-$C9H_2$-$C10H_2$ scissoring vibration. A new peak arises at 1576 cm^{-1}.

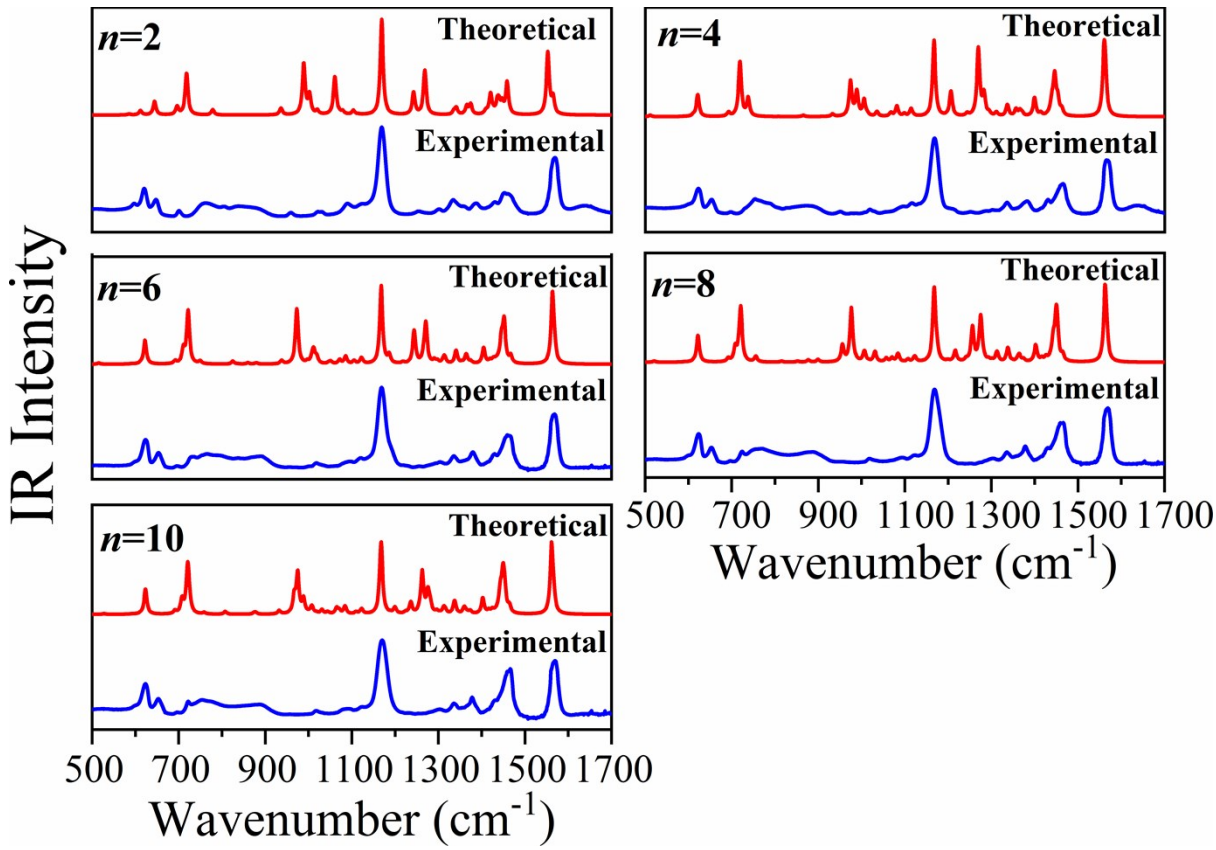

Fig. S5 Comparison of experimental and theoretical IR absorption spectra of the most stable geometries for the $C_n$mim Cl (n = 2, 4, 6, 8, 10) ion-pairs in the range of 500-1700 cm^{-1}.

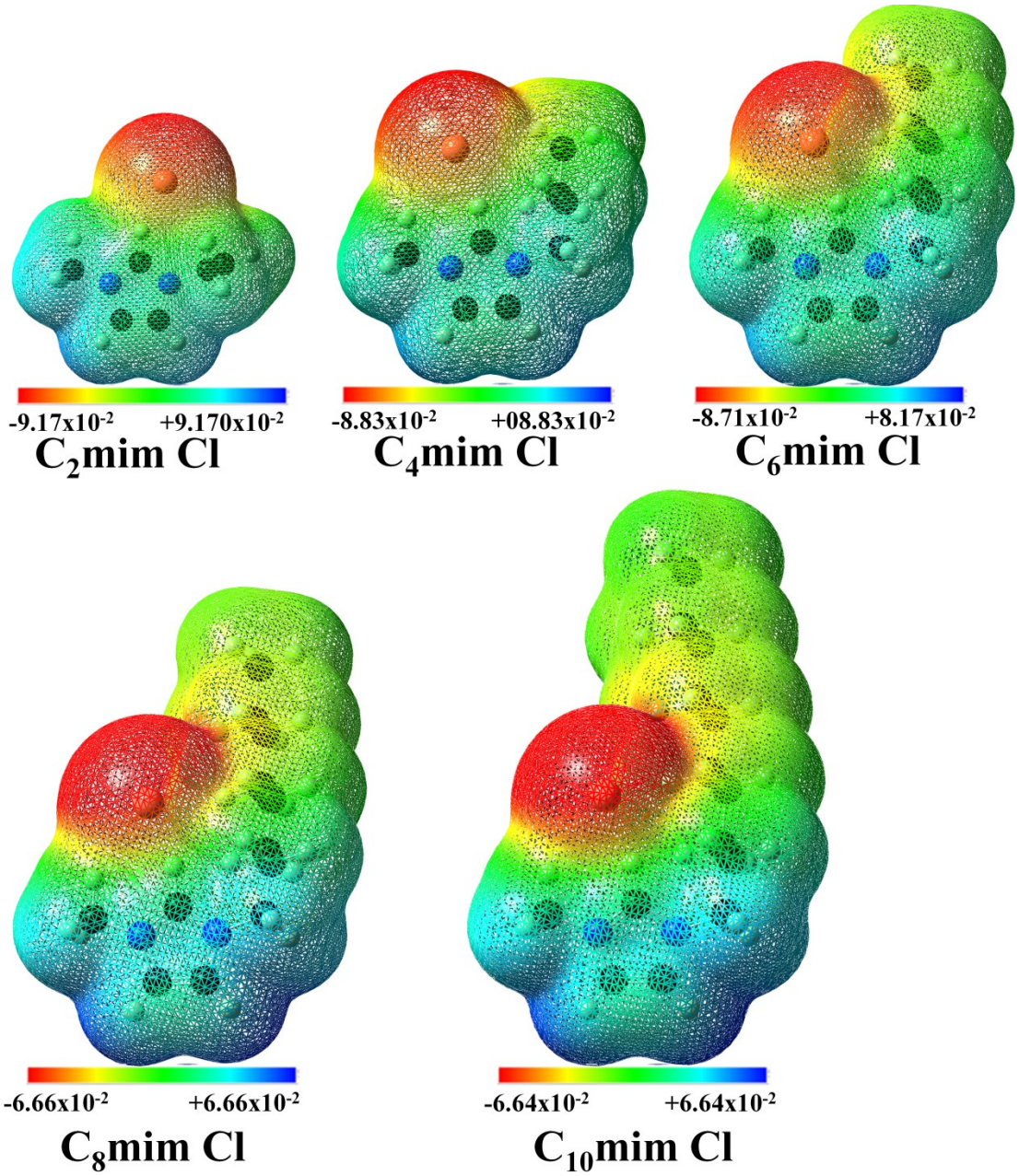

Fig. S6 Electrostatic potential mapping (ESP) from total self-consistent field (SCF) for $C_n$mim Cl (n = 2, 4, 6, 8, 10) ion-pairs.

Table S1. Bond lengths and dihedral angles of the optimized geometries of the $C_n$mim Cl (n = 2, 4, 6, 8, 10) ion-pairs obtained from the DFT calculations.

	C_2mim Cl	**C_4mim Cl**	**C_6mim Cl**	**C_8mim Cl**	**C_{10}mim Cl**
		Bond Length (Å)			
N1−C2	1.33	1.33	1.33	1.33	1.33
C2−N3	1.33	1.33	1.33	1.33	1.33
N3−C4	1.37	1.37	1.37	1.37	1.37
C4−C5	1.35	1.35	1.35	1.35	1.35
C5−N1	1.38	1.37	1.37	1.37	1.37
C2−H9	**1.12**	**1.12**	**1.11**	**1.11**	**1.11**
C5−H11	1.07	1.07	1.07	1.07	1.07
C4−H10	1.07	1.07	1.07	1.07	1.07
N1−C6	1.45	1.46	1.46	1.46	1.46
N3−C7	1.47	1.47	1.47	1.47	1.47
C6−H12	1.09	1.09	1.09	1.09	1.09
C6−H13	1.09	1.09	1.09	1.09	1.09
C6−H14	1.08	1.08	1.08	1.09	1.09
C7−H15	1.09	1.09	1.09	1.09	1.09
C7−H16	1.09	1.09	1.09	1.09	1.09
C8−H17	1.09	1.09	1.09	1.09	1.09
C8−H18	1.09	1.09	1.09	1.09	1.09
C9−H19	1.09	1.09	1.09	1.09	1.09
C9−H20		1.09	1.09	1.09	1.09
C10−H21		1.09	1.09	1.09	1.09
C10−H22		1.09	1.09	1.09	1.09
C10−H23		1.09	1.09	1.09	1.09
C11−H24			1.09	1.09	1.09
C12−H25			1.09	1.09	1.09
C12−H26			1.09	1.09	1.09
C13−H27				1.09	1.09
C13−H28				1.09	1.09
C14−H29				1.09	1.09
C14−H30				1.09	1.09
C14−H31				1.09	1.09
C15−H32					1.09
C15−H33					1.09
C16−H34					1.09
C16−H35					1.09
C16−H36					1.09
Cl20-H9	**1.99**	**2.00**	**2.02**	**2.02**	**2.02**
		Dihedral Angle (deg)			
∠ N1-C7-C8-C9		**-64.52**	**-64.54**	**-64.62**	**-64.73**

Table S2. Wavenumbers of vibrational modes for C_2mim^+ and the energetically optimized configuration of $C_n$mim Cl (n = 2, 4, 6, 8, 10), calculated using DFT and observed in the IR spectra.

Vibration	Computational		Experimental
	IR		
	C_2mim^+ (cm^{-1})	C_2mim Cl (cm^{-1})	
v_s (C4-H10, C5-H11)	3308 (10)	3279 (6)	3144 (W)
v_{as} (C4-H10, C5-H11)	3290 (16)		
v (C2-H9)	3292 (29)	2631 (1420)	3054 (S)
v_{as} (H12,13-C6- H14)	3189 (0.3)	3152 (1)	
v_{as} (H12-C6-H13)	3178 (0.1)	3132 (6)	
v_{as} (H15-C7-H16, H17,18-C8-H19)	3160 (8)	3124 (4)	2976 (M)
v_{as} (H15-C7-H16, H17,18-C8-H19)	3154 (5)	3115 (8)	
v_{as} (H15-C7-,H16); v_{as} (H17,18-C8-H19)	3138 (2)	3100 (14)	
v_s(H15-C7-H16)	3098 (6)	3055 (33)	2931 (W)
v_s (H12,13-C6-H14)	3085 (4)	3046 (22)	
v_s (H17-C8-H18,19)	3063 (4)	3020 (24)	2868 (W)

The C−H region for C_2mim Cl is scaled by 0.991. The IR intensities are shown in km/mol in parentheses. Key: W, weak; M, medium; S, strong; ν, stretch; ν_s, symmetric stretch; ν_{as}, asymmetric stretch.

Vibration	Computational		Experimental
	IR		
	C_4mim^+ (cm^{-1})	C_4mim Cl (cm^{-1})	
v_s (C4-H10, C5-H11)	3310 (10)	3134 (6)	3143 (W)
v_{as} (C4-H10, C5-H11)	3291 (19)		
v (C2-H9)	3292 (23)	2555 (1239)	3057 (M)
v_{as} (H12,13-C6- H14)	3177 (0.1)	2988 (7)	
v_{as} (H12-C6-H13)	3178 (0.1)	2971 (19)	
v_{as} (H21-22-C10-H12); v_{as} (H19-C9-H20)	3140 (16)	2958 (14)	2957 (S)
v_{as} (H15-C7-H16, H17-C8-H18)	3160 (8)	2950 (11)	
v_s (H19-C9-H20)	3125 (33)	2944 (43)	2930 (M)
v_{as} (H17-C8-H18), v_{as} (H21,22-C10-,H23); v_{as} (H19-C9-H20)		2929 (18)	
v_s(H15-C7-H16); v_{as} (H17-C8-H18); v_{as} (H19-C9-H20); v_{as} (H21,22-C10-,H23)	3102 (19)	2908 (9)	
v_s(H15-C7-H16); v_{as} (H17-C8-H18);	3093 (3.3)	2900 (28)	
v_s (H17-C8-H18);		2884 (11)	
v_s (H12,13-C6-H14)	3085 (4)	2879 (65)	
v_s (H21-C10-H22,23)	3051 (22)	2870 (42)	2867 (M)
v_s (H17-C8-H18)	3046 (14)	2858 (45)	
v_s (H19-C9-H20)	3030 (20)		

The C−H region for C_4mim Cl is scaled by 0.954. The IR intensities are shown in km/mol in parentheses. Key: W, weak; M, medium; S, strong; ν, stretch; ν_s, symmetric stretch; ν_{as}, asymmetric stretch.

Vibration	Computational		Experimental
	IR		
	C_6mim^+ (cm^{-1})	C_6mim Cl (cm^{-1})	
v_s (C4-H10, C5-H11)	3310 (10)	3054 (2)	3140 (W)
v_{as} (C4-H10, C5-H11)	3292 (17)	3036 (6)	
v (C2-H9)	3291 (25)	2526 (1128)	3052 (M)
v_{as} (H12,13-C6- H14)	3189 (0.4)	2919 (7)	
v_{as} (H25-C12-H26,27); v_{as} (H23-C11-H24)	3178 (0.2)	2900 (21)	2955 (M)
v_{as} (H15-C7-H16, H17-C8-H18)	3151 (4.2)	2880 (16)	
v_{as} (H25-C12-H26)	3130 (25)	2879 (37)	
v_s (H23-C11-H24), v_s (H21-C10-H22)	3118 (48)	2869 (61)	2929 (S)
v_s(H15-C7-H16); v_{as} (H17-C8-H18); v_{as} (H19-C9-H20), v_{as} (H21-C10-H22)	3103 (30)		
v_{as} (H17-C8-H18); v_{as} (H19-C9-H20),		2860 (34)	

v_{as} (H21-C10-H22)			
v_{as} (H17-C8-H18); v_{as} (H19-C9-H20), v_{as} (H21-C10-H22); v_{as} (H23-C11-H24); v_{as} (H25-C12-H26)		2849 (6)	
v_s(H15-C7-H16); v_{as} (H17-C8-H18); v_{as} (H19-C9-H20), v_{as} (H21-C10-H22); v_{as} (H23-C11-H24); v_{as} (H25-C12-H26)		2837 (4)	
v_s(H15-C7-H16)	3093 (7)	2831 (28)	
v_{as} (H23-C11-H24), v_{as} (H21-C10-H22)	3083 (36)	2830 (10)	
v_s (H18-C8-H19)	3046 (17)	2815 (11)	
v_s (H12,13-C6-H14)	3085 (4)	2810 (75)	
v_s (H25-C12-H26)	3045 (24)	2802 (41)	2857 (M)
v_s (H23-C11-H24); v_s (H19-C9-H20)	3034 (60)	2788 (77)	

The C−H region for C_6mim Cl is scaled by 0.923. The IR intensities are shown in km/mol in parentheses. Key: W, weak; M, medium; S, strong; ν, stretch; ν_s, symmetric stretch; ν_{as}, asymmetric stretch.

Vibration	Computational		Experimental
	IR		
	C_8mim^+ (cm^{-1})	C_8mim Cl (cm^{-1})	
v_s (C4-H10, C5-H11)	3310 (10)	3180 (2)	3141 (W)
v_{as} (C4-H10, C5-H11)	3291 (20)	3160 (6)	
v (C2-H9)	3292 (21)	2637 (106)	3055 (W)
v_{as} (H12,13-C6- H14)	3189 (0.4)	3038 (7)	
v_{as} (H12-C6-H13)	3177 (0.2)	3018 (22)	
v_{as} (H15-C7-H16, H17,18-C8-H19)	3152 (4)	2997 (16)	
v_{as} (H29,30-C14-H31)	3126 (30)	2990 (46)	
v_{as} (H29,30-C14-H31); v_{as} (H27-C13-H28)	3114 (56)	2986 (69)	2956 (M)
v_s(H15-C7-H16); v_{as} (H17-C8-H18); v_{as} (H19-C9-H20), v_{as} (H21-C10-H22)	3104 (34)		
v_{as}(H15-C7-H16); v_{as} (H17-C8-H18); v_{as} (H19-C9-H20), v_{as} (H21-C10-H22); v_{as} (H23-C11-H24)		2979 (49)	
v_{as}(H15-C7-H16); v_{as} (H17-C8-H18); v_{as} (H19-C9-H20), v_{as} (H21-C10-H22); v_{as} (H23-C11-H24); v_{as} (H25-C12-H26); v_{as} (H27-C13-H28); v_{as} (H29,30-C14-H31)	3086 (80)	2970 (16)	
v_s(H15-C7-H16); v_{as} (H17-C8-H18); v_{as} (H19-C9-H20), v_{as} (H21-C10-H22); v_{as} (H23-C11-H24); v_{as} (H25-C12-H26); v_{as} (H27-C13-H28); v_{as} (H29,30-C14-H31)		2958 (20)	
v_s (H15-C7-H16, H17-C8-H18)		2948 (28)	
v_{as} (H23-C11-H24); v_{as} (H27-C13-H28)		2941 (2)	
v_s (H17-C8-H18);); v_{as} (H23-C11-H24); v_{as} (H25-C12-H26); v_{as} (H27-C13-H28)		2932 (19)	
v_s (H17-C7-H18)		2931 (5)	
v_s (H17-C8-H18)	3084 (4)	2924 (80)	2924 (S)
v_s (H29,30-C14-H31)	3042 (33)	2915 (39)	2853 (M)
v_s (H17-C8-H18);); v_s (H23-C11-H24); v_s (H25-C12-H26); v_s (H27-C13-H28)	3034 (101)		
v_s (H27-C13-H28)		2909 (60)	
v_{as} (H17-C8-H18)		2900 (44)	
v_s (H21-C10-H22); v_{as} (H23-C11-H24); v_s (H25-C12-H26); v_s (H27-C13-H28)		2899 (57)	
v_s (H21-C10-H22); v_s (H25-C12-H26)		2896 (0.4)	
v_s (H23-C11-H24)		2892 (15)	

The C−H region for C_8mim Cl is scaled by 0.960. The IR intensities are shown in km/mol in parentheses. Key: W, weak; M, medium; S, strong; ν, stretch; ν_s, symmetric stretch; ν_{as}, asymmetric stretch.

Vibration	Computational	Experimental

	$C_{10}im^+$ (cm^{-1})	IR $C_{10}mim$ Cl (cm^{-1})	
v_s (C4-H10, C5-H11)	3311 (10)	3180 (2)	3141 (W)
v_{as} (C4-H10, C5-H11)	32901(19)	3161 (6)	
v (C2-H9)	3292 (22)	2640 (1104)	3057 (W)
v_{as} (H12,13-C6- H14)	3189 (0.4)	3039 (7)	
v_{as} (H12-C6-H13)	3178 (0.2)	3018 (22)	
v_{as} (H15-C7-H16, H17-C8-H18)	3152 (4)	2998 (15)	
v_{as} (H33,34-C16- H35)	3123 (34)	2992 (45)	
v_{as} (H33,34-C16- H35); v_{as} (H31-C15- H32)	3113 (60)	2987 (70)	2955 (W)
v_{as}(H15-C7-H16); v_{as} (H17-C8-H18); v_{as} (H19-C9-H20); v_{as} (H21-C10-H22); v_{as} (H23-C11-H24)		2980 (57)	
v_s(H15-C7-H16); v_{as} (H17-C8-H18); v_{as} (H19-C9-H20); v_{as} (H21-C10-H22); v_{as} (H23-C11-H24); v_{as} (H25-C12-H26); v_{as} (H27-C13-H28); v_{as} (H29-C14-H30)	3103 (37)	2971 (26)	
v_s(H15-C7-H16); v_{as} (H17-C8-H18); v_{as} (H19-C9-H20); v_{as} (H21-C10-H22); v_{as} (H23-C11-H24); v_{as} (H25-C12-H26); v_{as} (H27-C13-H28); v_{as} (H29-C14-H30); v_{as} (H33,34-C16- H35); v_{as} (H31-C15- H32)	3087 (126)	2962 (72)	
v_s (H15-C7-,H16); v_{as} (H17,18-C8-H19)		2948 (28)	
v_{as} (H19-C9-H20), v_{as} (H21-C10-H22); v_{as} (H23-C11-H24); v_{as} (H25-C12-H26); v_s (H27-C13-H28); v_s (H29-C14-H30)	3034 (150)	2924 (80)	2922 (S)
v_s (H33,34-C16- H35)		2917 (39)	
v_s (H31-C15- H32)		2912 (78)	2852 (M)
v_s (H19-C9-H20), v_s (H21-C10-H22); v_s (H23-C11-H24); v_s (H25-C12-H26); v_s (H27-C13-H28); v_s (H29-C14-H30)	3034 (150)	2904 (83)	
v_s (H19-C9-H20)	3016 (4)	2902 (40)	

The C−H region for C_{10}mim Cl is scaled by 0.961. The IR intensities are shown in km/mol in parentheses. Key: W, weak; M, medium; S, strong; ν, stretch; ν_s, symmetric stretch; ν_{as}, asymmetric stretch.

Table S3. Natural bond orbital (NBO) electron density in the cation and four configurations of $C_n$mim Cl (n=2,4,6,8, and 10), calculated at the wB97XD/6-311++G(d,p) level of theory.

	C_2mim	C_2mim Cl	C_4mim	C_4mim Cl	C_6mim	C_6mim Cl	C_8mim	C_8mim Cl	C_{10}mim	C_{10}mim Cl
N1	-0.34	-0.37	-0.34	-0.36	-0.34	-0.36	-0.34	-0.36	-0.34	-0.36
C2	**0.30**	**0.28**	**0.29**	**0.27**	**0.29**	**0.27**	**0.29**	**0.27**	**0.29**	**0.27**
H9	**0.24**	**0.29**	**0.24**	**0.29**	**0.24**	**0.29**	**0.24**	**0.29**	**0.29**	**0.29**
N3	-0.34	-0.36	-0.34	-0.37	-0.34	-0.36	-0.34	-0.36	-0.36	-0.36
C4	-0.01	-0.02	-0.00	-0.03	-0.00	-0.03	-0.00	-0.03	-0.00	-0.03
H10	0.25	0.23	0.25	0.23	0.25	0.23	0.25	0.23	0.25	0.23
C5	-0.01	-0.04	-0.01	-0.03	-0.01	-0.03	-0.01	-0.03	-0.01	-0.03
H11	0.25	0.23	0.25	0.23	0.25	0.23	0.25	0.23	0.25	0.23
C6	**-0.36**	**-0.35**	**-0.36**	**-0.37**	**-0.36**	**-0.37**	**-0.36**	**-0.37**	**-0.36**	**-0.37**
H12	**0.23**	**0.21**	**0.23**	**0.20**	**0.23**	**0.20**	**0.23**	**0.20**	**0.23**	**0.20**
H13	0.23	0.21	0.23	0.20	0.23	0.20	0.23	0.20	0.23	0.20
H14	0.22	0.24	0.22	0.27	0.22	0.27	0.22	0.27	0.22	0.27
C7	**-0.17**	**-0.18**	**-0.17**	**-0.15**	**-0.16**	**-0.15**	**-0.16**	**-0.16**	**-0.16**	**-0.15**
H15	**0.21**	**0.26**	**0.22**	**0.20**	**0.22**	**0.21**	**0.22**	**0.20**	**0.22**	**0.20**
H16	0.22	0.19	0.22	0.21	0.22	0.20	0.22	0.20	0.22	0.20
C8	-0.59	-0.59	-0.40	-0.42	-0.39	-0.41	-0.39	-0.41	-0.39	-0.41
H17	0.21	0.24	0.20	0.24	0.20	0.21	0.20	0.21	0.20	0.21

H18	0.21	0.19	0.22	0.21	0.22	0.23	0.22	0.23	0.22	0.23
H19	0.23	0.21	0.18	0.18	0.19	0.18	0.18	0.18	0.18	0.18
C9			-0.39	-0.39	-0.39	-0.38	-0.39	-0.39	-0.39	-0.38
H20			0.18	0.20	0.18	0.20	0.18	0.20	0.19	0.20
C10			-0.27	-0.58	-0.38	-0.39	-0.38	-0.39	-0.38	-0.39
H21			0.20	0.18	0.19	0.17	0.20	0.17	0.20	0.17
H22			0.21	0.24	0.19	0.23	0.19	0.23	0.19	0.23
C11					-0.38	-0.38	-0.38	-0.38	-0.37	-0.37
H23			0.21	0.20	0.18	0.17	0.19	0.17	0.19	0.17
H24					0.19	0.20	0.20	0.20	0.19	0.20
H25					0.19	0.19	0.19	0.18	0.18	0.18
C12					-0.57	-0.57	-0.38	-0.38	-0.38	-0.37
H26					0.20	0.18	0.18	0.20	0.18	0.20
H27					0.21	0.20	0.19	0.18	0.19	0.19
C13							-0.38	-0.38	-0.37	-0.37
H28							0.19	0.19	0.18	0.19
H29							0.19	0.19	0.20	0.19
C14							-0.57	-0.57	-0.38	-0.38
H30							0.19	0.19	0.19	0.18
H31							0.19	0.19	0.19	0.19
C15									-0.38	-0.38
H32									0.18	0.18
H33									0.19	0.18
C16									0.18	0.19
H34									-0.57	-0.57
H35									0.19	0.19
Cl38		**-0.86**		**-0.86**		**-0.86**		**-0.86**		**-0.86**